

Design and Manufacturing an Explosive Ordnance Disposal Robot Chassis

[†]Radian A. Gondokaryono, [†]Priadi Teguh Wibowo, [†]Yusuf Salman, [†]Putra Agung, [†]Aris Budiarto, and [‡]Agus Budiyo

[†]Bhimasena Research, Technology and Development, Sumedang, Indonesia

[‡]School of Aerospace, Mech. and Manufacturing Eng. Aerospace and Aviation Program, RMIT University, Melbourne, Australia

Abstract—This paper describes the development of a lightweight chassis and drivetrain of an Explosive Ordnance Disposal Robot. It defines the design methodology of selecting the correct specification of a robot to define a general concept of the robot. The chassis and drivetrain movement concept is described and a finite element analysis is achieved to validate the strength of the robot under intermediate payloads.

Keywords—EOD robot, rotating track transmission, payload chassis, structural analysis.

I. INTRODUCTION

DURING the past years, robots have increased in popularity for explosive ordnance (EOD) missions. Advancing technologies have made it possible for robots to function as a replacement for humans in high risk situations. This reduced risk is a primary advantage of developing a particular robot specifically tailored for EOD missions. Robots are now able to manipulate surroundings, traverse various terrains in urban and wild environments.

Our research is now interested in designing a robot chassis to perform functions in EOD missions.

II. DESIGN METHODOLOGY

To achieve the desired functionality of the robot, the procedure starts with benchmarking of other robots [1]-[2], determining design requirements and objectives (DRO), concept design, preliminary design, and structural analysis. Basic concept is determined by integral mechanical and electrical solutions to the problem at hand. The control scheme of electrical parts, sizes, and weights determine the required mechanical supporting parts and vice versa. A mechanical challenge of having a rotating track frame which also transmits torque is overcome.

A. Benchmarking

For a starting point, robots that are already on the market are compared. A main point is that most robots of this size have a

rotating track with 5 kg payload. **TABLE I** is a summary of these comparisons.

B. Design Requirement and Objectives

From benchmarking and based on the functions needed for our applications of this robot, the design requirement and objectives is determined.

TABLE I DESIGN REQUIREMENTS AND OBJECTIVES

Chassis		Wheeldrive		Manipulator	
Dimension (H)	45 cm	Motor	Brush DC	Degree of Freedom	5-DOF
Dimension (W)	60 cm	Speed	9 kmh	Joint Rotation	120 deg
Dimension (L)	70 cm	Drive model	2 motor	Vertical Reach	160 cm
Weight	45 kg	Climb Elevation	30 degree	Horizontal Reach	160 cm
Payload Bays		Vertical Obstacle	20 cm	Weight	15 kg
Protection	-	Clearance	3 cm	Lift Capacity (Close)	-
Track	49.5 cm	Configuration	Front Tracks	Lift Capacity (Ext.)	7 kg
Rotating Track	29.43cm	Track Length	25 cm	Clamp Opening	20 cm
Safety Factor	1.5	Rotation	Continuous		

III. OVERALL CONCEPT DESIGN

To meet the design requirements and objectives, this robot uses brush DC motors assembled to planetary gearboxes. The drivetrain is completed with a main track, rotating track, and rubber wheels. The main track and rotating track are used to climb up stairs and obstacles with an inclination angle. The rotating tracks (tracks that can change angles of attack with continuous rotation) are shown at the front of the robot.

The robot arm has 5 degrees-of-freedom (DoF) equipped with horizontal fixed camera and a pan/tilt camera. The arm has a desired 7 kg payload at full extension.



Figure 1 Overall concept drawing of the robot

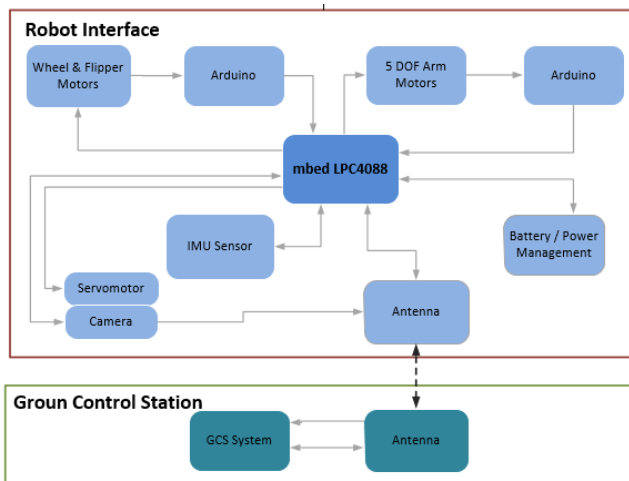


Figure 2 Electronics system

Figure 2 shows the electronics system of the robot. The main controller of this robot is mbed LPC4088 with auxiliary controller, Arduino acting as bridge to motor driver. The Arduino gives speed command and retrieve information about motor angle and speed. The mbed also communicates with IMU sensor to get the altitude and direction information and with Smart Battery to control the battery and collect battery condition information. There are three cameras whose motion is controlled by servomotor. The servomotor itself is commanded by the mbed. Lastly the main controller communicates with the host PC through transceiver to exchange information.

IV. POWER TRANSMISSION DESIGN

A. Concept

The power transmission of this robot has 3 degrees-of-freedom, left movement (track, rotating track, front wheel, and back wheel), right track movement, and rotating

track frame rotation. Figure 3 shows the main track concept. Each side is actuated by one motor placed at the back of the robot combined with right angle bevel-planetary gearbox. This gearbox moves the main track by the back sprocket and is connected to a front sprocket. The front sprocket then moves the rotating track sprocket by bolted connection. The rotating track then drives the outer rotating track sprocket which drives the front wheel of the robot. The back wheel is connected to the back sprocket. This results in front back drive driven by the back sprocket. Each side, left and right is driven by this mechanism.

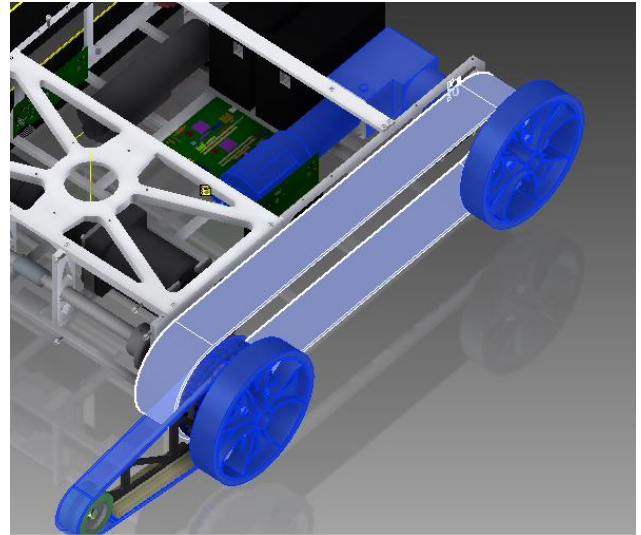


Figure 3 Main track concept

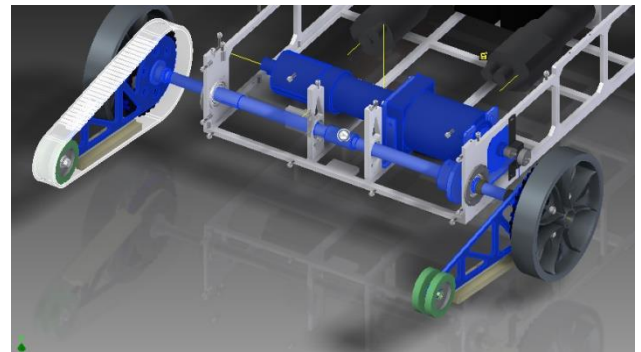


Figure 4 Rotating track transmission

The 3rd DOF is the movement of the angle of rotating track of robot to function as a climbing mechanism and also as a support of lifting weight to prevent the robot from rolling over while lifting the payload as in [3]. Because the rotating track frame has continuous rotation, this mechanism is also used to elevate the robot chassis from the ground to achieve higher field of view. Figure 4 shows the rotating track transmission concept.

The rotation of this frame is connected to a front drive shaft that is inner to the main track wheel. This shaft connects the right and left tracks to move in tandem and is driven by a brush DC motor connected with a planetary gearbox. The front drive

shaft also functions as the main axle support of the front track/wheel.

B. Motor and Gearbox Selection

For a selection of motors, the most extreme torque case is defined when the robot is climbing an inclination of 30 degrees. The free body diagram is shown in **Figure 5**.

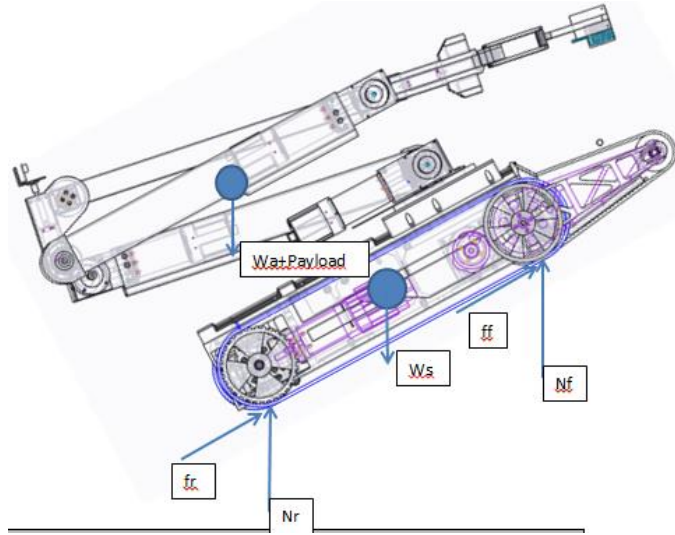


Figure 5 Inclination free body diagram

TABLE II RESULTING FORCES

Inclination FBD			
Inclination angle	Θ	30	degrees
Front Normal force	N_f	366	N
max Front friction force	f_f	256	N
Rear Normal Force	N_r	15	N
max Rear friction force	f_r	11	N
Total force to overcome inclination	F	220	N
Wheel FBD Full Rear Load			
front friction if full rear load	ff_1	209	N
	$ff_1 < f_r$ ok?	ok	
Rear Torque	T_r	0.9	Nm
Front Torque	T_f	19	Nm
Total Required Torque for 1 motor	$T_m = (T_r + T_f)/2$	10	Nm
Efficiency	E	85	%
Total Torque	T_{me}	12	Nm
Wheel FBD Full Front Load			
Rear friction if full front load	f_r	-36	
	$ff_1 < f_r$ ok?	ok	
Rear Torque	T_r	-3	N
Front Torque	T_f	23	
Total required Torque for 1 motor	T_m	10	Nm
Total Torque	T_{me}	12	Nm

TABLE II concludes that each side motor should achieve a minimal 12 Nm torque to overcome a 30° inclination. Next is motor and gearbox selection. We chose a Maxon motor with .345 Nm at 3500 rpm attached to a 1:40 planetary bevel gearbox as described in [4, 698, 706-707]. The total output

torque then is 14 Nm and the maximum speed, with a 7 in wheel, is 9 km/h.

C. Preliminary

The overall components of the drivetrain design can be divided into the front drivetrain and the back drivetrain. The front drivetrain implements both track wheel movements and rotating track rotation movement. Design uses manufacturing capabilities of CNC milling and turning for axle parts. With these two manufacturing methods, there should be enough precision for the functionality and efficiency of the robot. Materials used are aluminum dural 7075 t6 for frames and stainless steel 420 or AISI 1045 for axles.

Figure 6 shows the full assembly of the drivetrain/chassis of the robot. Important parts are the rotating track frame (71), driveshaft flange (9), and driveshaft (27).

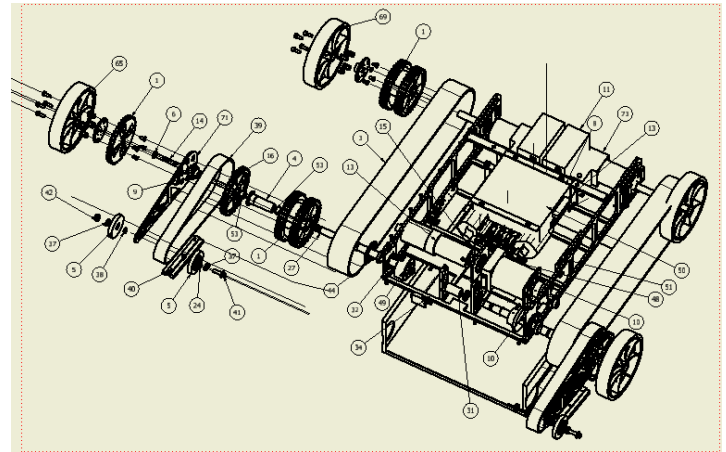


Figure 6 Robot assembly

D. Weight and Balance

From a detailed assumption of the weights of all the parts of the robot, the center of gravity is calculated to check whether the robot will turn over. This happens when the resulting normal force on the wheels is negative. The robot is checked for when lifting the weight at full extension, at the ready position with payload, and ready position during a 30 degree inclination. The Free Body diagram and resulting loads are shown in **Figure 7** and **TABLE III**.

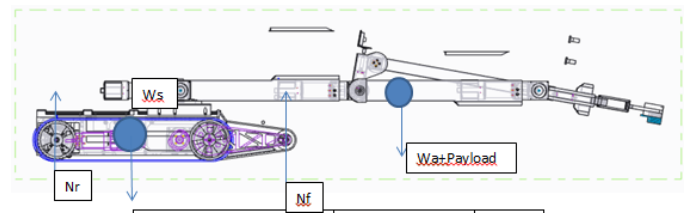


Figure 7 Full extension free body diagram

E. Structural Analysis

The structural analysis of the robot is analyzes the most extreme load case which is when the robot lifts a weight of 15kg at full extension 1.6 Nm. With these calculations, the forces on the front of the rotating tracks and the rear wheels can be determined. The next figure shows the force diagram on the robot during the lift case.

TABLE III FREE BODY DIAGRAMS RESULTING LOADS

Case	Load Table		
	Load	Value	Unit
Full Extension	W _a + payload	263	N
	W _s	255	N
	N _f	612	N
	N _r	0	N
Ready Position	W _a + payload	263	N
	W _s	255	N
	N _f	182	N
	N _r	336	N
30° Inclination	W _a + payload	263	N
	W _s	255	N
	N _f	111	N
	N _r	338	N

It is expected that the rotating track mechanism is the main supporting parts for the front drivetrain. The critical part shown below is the rotating track frame to support the weight of the robot and as a support for the rotating tracks. A maximum inertia design with optimal weight is achieved by concept of mechanical trusses.

Figure 8 shows the rotating track frame is loaded with a vertical force of 306 N and an assumed side force of 50 N (for when the robot turns). The resulting stresses is a reaction force and moment at fixed constraint.

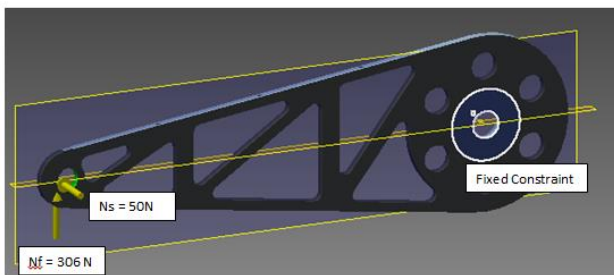


Figure 8 Rotating track frame load constraints

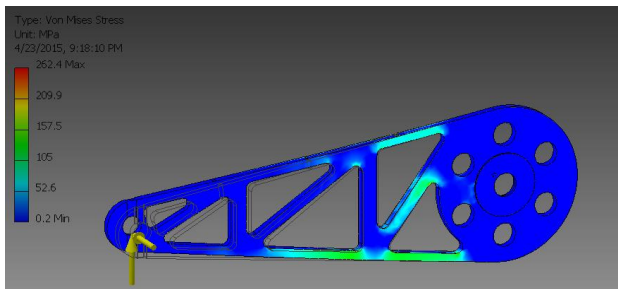


Figure 9 Rotating track frame stress distribution

Figure 9 shows the internal stress of the rotating track frame which is adequately distributed throughout the part. The maximal Von-misses stress is 262.4 MPa. In relationship to the materials yield strength, the part has a Safety Factor of 2.5. A

lower SF can be achieved by thinner material (<5mm) but will comprimize the horizontal rigidity of the part.

Next is the connecting and driving part of the rotating track frame which is the drive shaft. This driveshaft also connects the left and right rotating tracks and is a bearing support for the front drivetrain assembly. The driveshaft is a standard hollow axle design for maximum inertia with splines at the end for a high torque mechanical connection. It is designed so it can be assembled from the outer frame.

Here is the theory of maximum stress on a shaft under tosion load as in [4, 101]:

$$\tau = \frac{Tr}{J} \quad (1)$$

where τ is maximal stress on shaft, T is torque, r is shaft radius, and J is moment of inertia.

The maximum load case is when the arm payload is at full extension. The driveshaft experiences a moment of 67 Nm from both left and right rotating tracks, an axial load 306 N, and sprocket chain tension of 4000 N as shown in Figure 10. The constraints are a sliding bearing constraint and a tangential constraint for the sprocket holding the torque. The drive shaft is calculated by structural theory as described in Equation (1) to save iteration time and is validated by finite element analysis for stress concentrations on the detailed drive shaft.

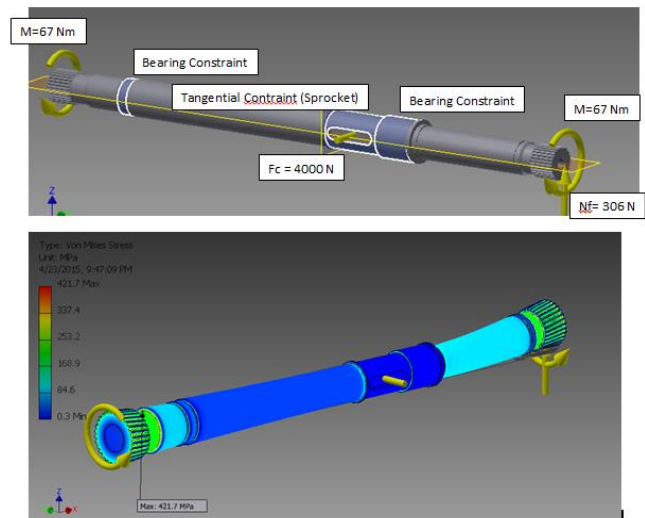


Figure 10 Driveshaft constraints and stress distribution

The stress distribution in Figure 10 is adequately uniform. The max von misses stress is 421 MPa at the spline gear step. With a stainless 420 material, this part has a Safety Factor of 1.2.

The next part that is critical to design is the spline hub connection between the driveshaft and the rotating track frame flange. The forces here are a moment torque of 67 Nm and a radial load of 306 Nm. The spline hub connection design is precalculated by hand to save iteration time.

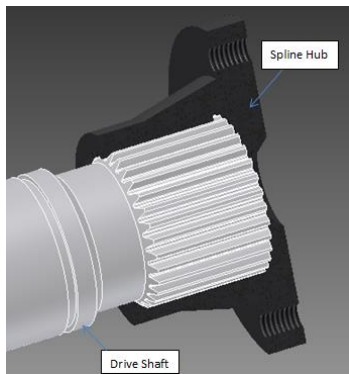


Figure 11 Spline connection

The stress analysis setup, **Figure 11** and **12**, is the same as the drive shaft, the difference is an assembled flange. A sliding contact connection is defined between the gear teeth and hub to accommodate for bending of the tooth. With bonded connections, the tooth fails with stress concentrations.

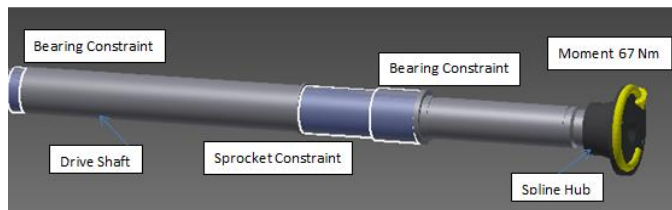


Figure 12 Spline connection analysis constraints

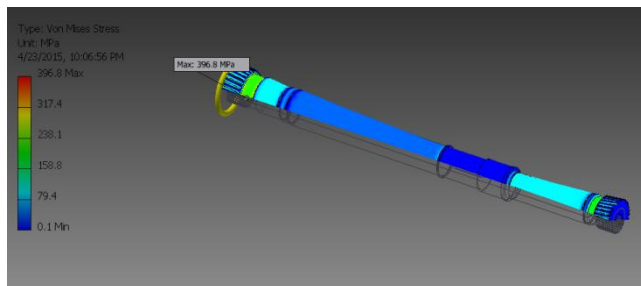


Figure 13 Spline connection stress distribution on shaft

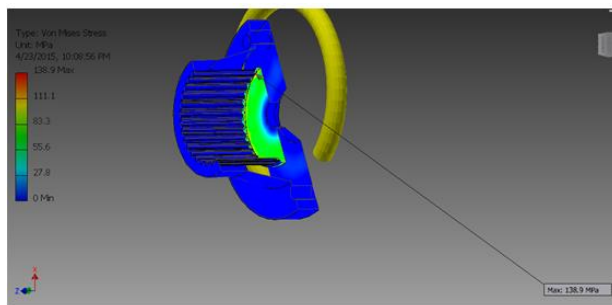


Figure 14 Spline connection stress distribution on hub

Figure 13 illustrates the same uniform stress distribution as the drive shaft of the previous analysis. The maximum von misses stress is 396.8 MPa at the same location as resulted in the drive shaft analysis because some energy is used to deform the tooth and flange.

Figure 14 illustrates the maximum Von-misses stress of the hub flange to be 136.9 MPa.

V. CHASSIS DESIGN

A. Concept

The robot chassis is manufactured with Aluminum Dural 7075 enclosed with carbon fiber body. The chassis supports full arm weight at full extension, supports various robot components including gearbox, motors, electronics, etc. It also has a main track tensioner mechanism.

B. Structural Analysis

The chassis is designed for a full extension payload weight of 15 kg for future upgrades of the arm lifting capacity as shown in **Figure 15**, the chassis is loaded with arm weight and torque and various chassis components weights. The constraint is a fixed constraint at bearing location.

The maximum Von-misses stress in **Figure 16** is 314.3 MPa at the location of the arm joint. With a material of Aluminum 7075 t6, the final weight of the chassis is 3.74 kg with bolts and nuts and has a Safety Factor of 1.4 (well within design requirements).

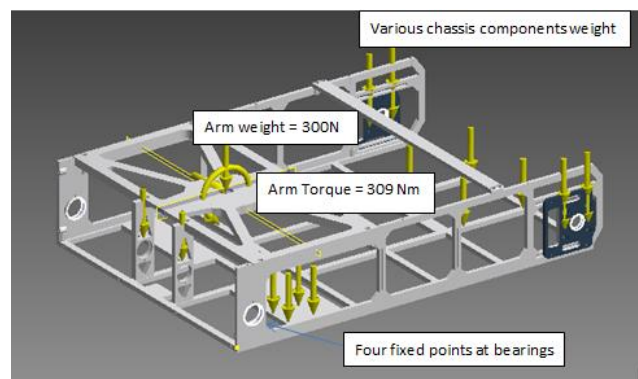


Figure 15 Chassis analysis setup

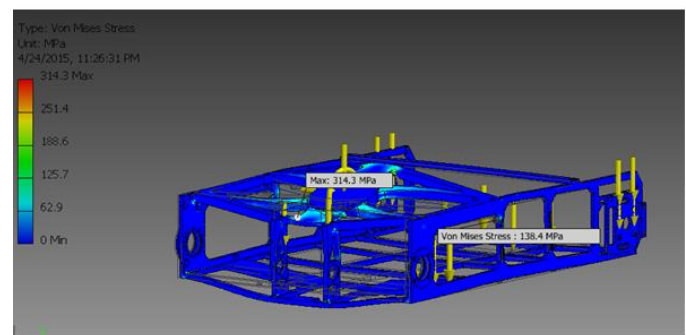


Figure 16 Chassis stress distribution

VI. MANUFACTURING

The robot chassis is Aluminum 7075 t6 manufactured with CNC milling and bolt connections. The drivetrain is mainly steel with turning manufacturing and fitter finishing for bearings.

The robot chassis/drivetrain in **Figure 17** is fully assembled with tracks and track rotation. The resulting chassis is made within tolerances and the structure is rigid to mount gearboxes.

The front axles and back axles are rigid to chassis and freely rotate with little friction. Most friction is assumed to be from track tension as without tracks the track sprockets rotate freely.

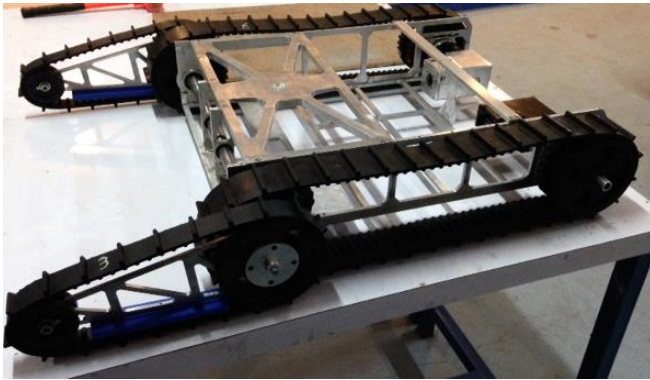


Figure 17 Manufactured robot

VII. CONCLUDING REMARKS

An explosive ordnance robot chassis/drivetrain has been designed and manufactured with off the market motor and gearbox selection, theory hand calculations, weight and balance calculations, production design, and finite element analysis.

REFERENCES

- [1] K. Chuengsatiansup and K. Sajjapongse, et al. "Plasma-RX: Autonomous Rescue robots," in *Robotics and Biomimetics, 2008. ROBIO 2008. IEEE International Conference* pp. 1986-1990, 22-25 Feb. 2009 [CrossRef](#)
- [2] Nima Enayati, Farid Najafi, (2011) "Design and manufacturing of a tele-operative rescue robot with a novel track arrangement", *Industrial Robot: An International Journal*, Vol. 38 Iss: 5, pp. 476 - 485. [CrossRef](#)
- [3] Wolf Y, inventor; Driving flipper with robotic arm. US patent 20130270017 A1. October 13, 2013.
- [4] R. Budynas, Shigley's Mechanical Engineering Design, 9th ed., McGraw-Hill, 2011.